Simulation and Implementation of a Mach-Zender Interferometer-Based Thermo-Optic Switch

Timothy Perrier

***Abstract*—This paper reports on the design and experimental implementation of a Mach-Zender Interferometer (MZI) exhibiting thermo-optic switching characteristics. This MZI has a 3.1 nm free spectral range (FSR) and the switching occurs with a 25°C temperature increase. In addition, the effect of path length difference is investigated through the comparison of two different MZIs.**

***Index Terms*—Mach-Zender Interferometer, thermo-optical effect, optical switching**

I. Introduction

Traditionally, the use of silicon-on-insulator (SOI) foundries has been widely used for development of CMOS devices. However, in 2004 a rapid shift occurred, and these SOI foundries began being used for optoelectronic integration as well. Having this CMOS fabrication compatibility made it easy to develop optical devices such as MZI switches and optical circuit integration [1].

Mach-Zender Interferometers (MZI) are important building blocks in SiPh integrated circuits due to their unique functionality of interfering signals. A classic MZI splits an incident light beam into two arms, and the light recombines at the output. Figure 1 depicts the general structure of an MZI based on Y-branches. Varying parameters of the MZI such as path length difference results in varying degrees of constructive or destructive interference at the output as a result of phase changes. Temperature changes in the arms of an MZI also affect light interference at the output by inducing a phase change of the light signal. This phase change comes as a result of the refractive indices of materials to vary depending on temperature. Using this thermo-optic effect, an MZI can be designed and used as an optical switch by having a temperature change that induces a π phase shift of the signal in one arm.

This report aims to investigate the effects of path length difference and temperature changes on various MZI structures and how an MZI can be used as a thermo-optic switch. Parameters such as the FSR, extinction ratio, and the temperature change required for π phase shift will be analyzed and compared to simulated results.

II. Design of the MZI

The waveguides for these devices follow the buried waveguide structure. It consists of a 500 nm by 220 nm silicon core and a cladding oxide surrounding the core. To design these MZI switches, the key parameter to focus on is the path length difference (ΔL) between the two arms. For different desired values of Free Spectral Range (FSR), there are varying ΔL values. This relationship can be observed in equation 1, which can be rearranged into equation 2.

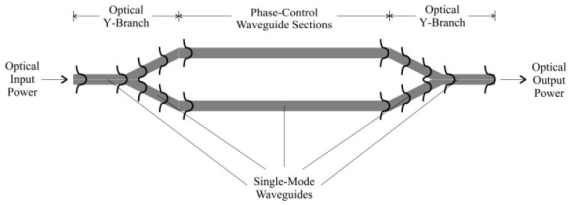

Fig. 1. General structure of an MZI with Y-branches at the input and outputs [2].

$$FSR = \frac{\lambda^2}{n_g \Delta L} \tag{1}$$

$$\Delta L = \frac{\lambda^2}{n_g FSR} \tag{2}$$

The *ng* values are obtained from Lumerical MODE simulations. The waveguide used has a width of 500 nm so at a wavelength of 1550 nm, the corresponding *neff* and *n*g values are 2.442 and 4.202, respectively. Desired FSR values for the ΔL calculations are 2.4, 4.8, and 9.6 nm. Therefore for TE mode, the MZI should have path lengths of 238, 119, and 59.6 μm.

To obtain the ON/OFF switching mechanism in an MZI, the temperature change must result in a π phase shift as seen from equation 3 below. To obtain this π phase shift, the ΔL must be changed from the values calculated previously. The Δ*neff* value is obtained from a Lumerical MODE script provided by the EDX course. For TE mode Δ*neff* is 0.0002, and for TM mode Δ*neff* is 0.0011. Then using equation 3, the ΔL for TE should be 390.8 μm and ΔL for TM should be 710.4 μm. The effect of temperature change on the transmission spectra of the MZI can be observed in Figure 2, where the blue and green curves are transmission at 25°C and 30°C, respectively. Increasing the temperature difference will shift the green curve further to the right of the blue curve.

$$\Delta\beta * \Delta L = \frac{2\pi}{\lambda} \Delta n_{eff} * \Delta L = \pi \tag{3}$$

$$\Delta T = \frac{\lambda}{2L\frac{dn}{dT}} \tag{4}$$

T. Perrier is with the Department of Electrical and Computer Engineering, McGill University, Montreal, QC, H3A 0E9 CA (e-mail: timothy.perrier@mail.mcgill.ca)

Manuscript received April 23, 2021.

Obtaining the value of the required temperature shift to achieve a π phase shift follows equation 4. Using $1.87*10^{-4}$ for $\frac{dn}{dT}$ yields a result of ΔT being 20.72°C. This version of the equation assumes that ΔL is 0, so the value for an MZI with a nonzero ΔL will be different.

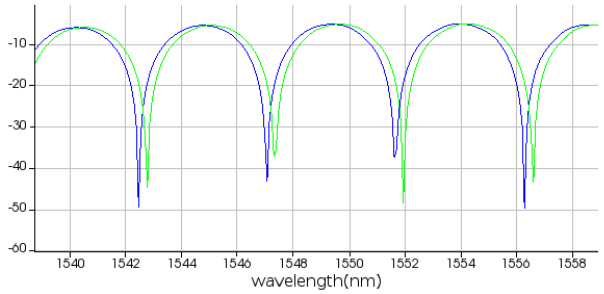

Fig. 2. A graph showing the dependence of transmission on temperature of the simulated MZI. The blue curve is transmission at 25°C, and the green curve is transmission at 30°C.

Values of ΔL used for these MZI structures are 27.63, 77.6, 196.07, 437.44, and 602.99 μm. These values vary from the ones calculated above.

The MZI devices were fabricated with 100 keV E-Beam lithography using the JEOL JBX-6300FS.

III. Experimental Results

The MZI structure designed as the thermo-optic switch can be seen in Figure 3. This particular MZI has a ΔL of 169.07 μm and is labeled as "MZI6". The MZI devices for TE mode were tested at temperature values of 25°C, 35°C, and 50°C. From simulations and Figure 3, the wavelength dependence on temperature was found to be approximately 0.06 nm/°C.

Parameters including the total insertion loss (TIL), delay line loss, and the extinction ratio are listed in Table I. To determine the loss from different elements in the MZI, a loopback structure consisting of two VGCs and a waveguide was designed and tested. This loopback structure's waveguide has approximately the same length as the L1 of the MZI. Obtaining the delay line loss of the MZI is done by comparing the outputs of the MZI to the output of the loopback structure. Since the delay line loss is not a significant portion of the TIL, we can infer that majority of the losses come from the VGCs. Unfortunately, there were no structures to test the loss from VGCs or Y-branches individually. The extinction ratio of MZI6 at a wavelength of 1550 nm is 19.66 dB, and the extinction ratio of MZI4 is 24.18 dB. Their FSR values differ greatly as well, being 3.1 nm for MZI6 and 7.36 for MZI4.

TABLE I
Table of MZI Parameters

	MZI6	MZI4
Total Insertion Loss	39.7166 dB	30.1634 dB
Delay Line Loss	9.5532 dB	3.9476 dB
Extinction Ratio	19.66 dB	24.18 dB
FSR	3.1 nm	7.36 nm

The device analyzed in detail in this section is labeled as "MZI6" and has a ΔL of 169.07 μm. Figure 4 compares the transmission spectrum of MZI6 at 25°C with the transmission at 35°C and 50°C separately. Figure 5 shows a zoomed in view of the transmission at all three temperatures. From this set of graphs, a wavelength shift can be distinguished as the temperature increases. With an increase of 10°C the shift is 0.76 nm, and an increase of 25°C corresponds to a 1.63 nm shift. Using these wavelength shifts, the wavelength dependence on temperature can be defined as approximately 0.07 nm/°C which is very close to the simulated value of 0.06 nm/°C. At 50°C, the π phase shift can be observed, and at 35°C the phase shift is approximately π/2. Looking back to the calculation result of equation 4 with ΔT being 20.72°C, we can see that the experimental 25°C shift is not far off. As mentioned previously, the result from equation 4 does not consider a path length difference which is why these results are not exactly the same.

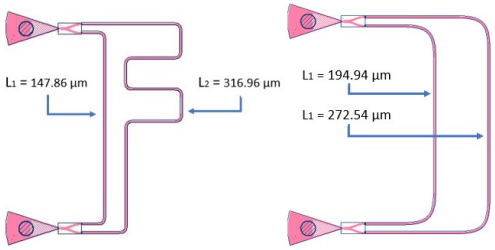

Fig. 3. (Left) A schematic of the "MZI6" structure used as a thermo-optic switch. (Right) A schematic of the "MZI4" structure used to compare the effects of path length difference on transmission.

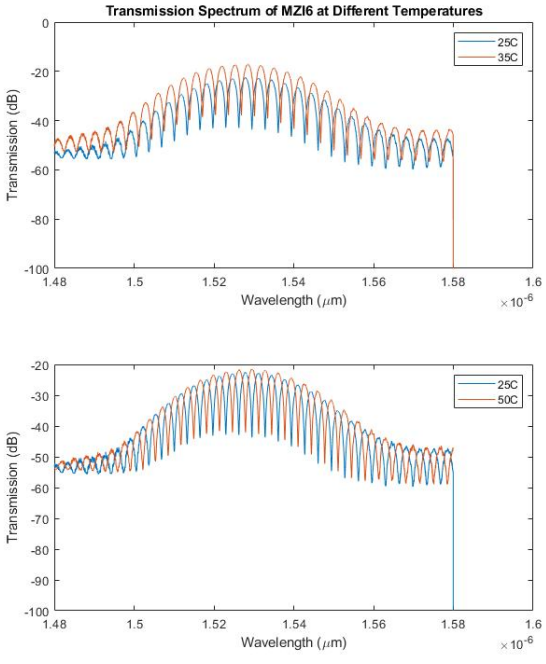

Fig. 4. (Top) Graph comparing the transmission versus wavelength of MZI6 at 25°C and 35 °C. (Bottom) Graph comparing the transmission versus wavelength of MZI6 at 25°C and 50 °C.

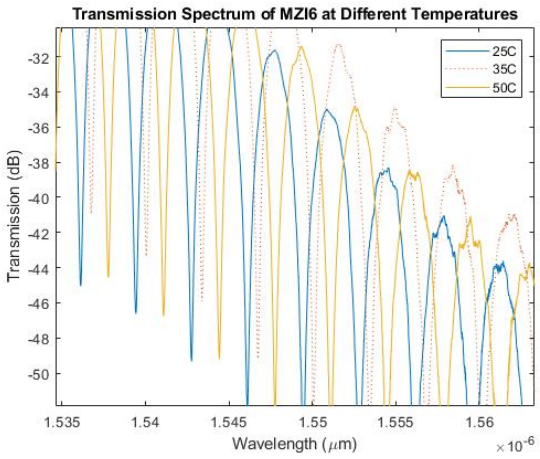

Fig. 5. Zoomed in view of a graph comparing the transmission versus wavelength of MZI6 at 25°C, 35°C, and 50°C.

Figure 6 compares the transmission of two MZI devices that have different path length differences. The MZI labeled "MZI6" has a path length difference of 169.07 μm, and the MZI labeled "MZI4" has a path length difference of 77.6 μm. The two MZI devices can be seen side-by-side in Figure 3 where the one on the left is MZI6, and the one on the right is MZI4. We can also see that MZI4 has a larger bend radius for the path of L2. From Figure 6, we can see that the FSR of MZI4 is much larger than that of MZI6.

IV. Discussion and Conclusion

When comparing the simulated results to the experimental results, we can see many similarities. The simulation uses a different path length difference being 100 μm rather than the 169.07 μm used for MZI6; however, the overall results are still close. The simulation resulted in a thermal tuning efficiency of 0.06 nm/°C whereas MZI6 shows only a 0.01 difference at 0.07 nm/°C. The temperature increase required for a π phase shift is also similar between the simulation and experimental results. From the simulation, the $\Delta T\pi$ is 20.72°C which is approximately 4°C lower than the experimental result of 25°C. The simulation uses different path length values which contributes to this difference.

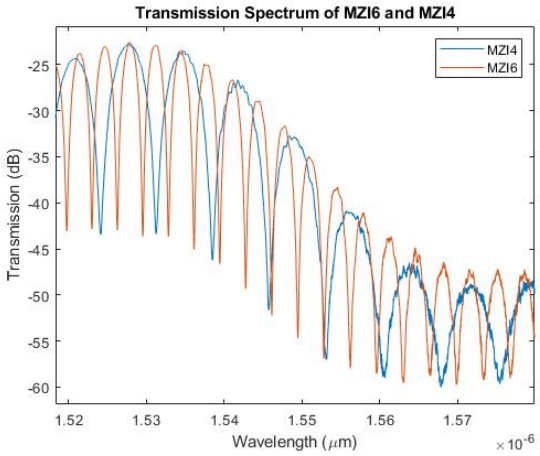

Fig. 6. A graph showing the transmission spectra of MZI4 and MZI6 versus wavelength. MZI4 has a path length difference of 77.6 μm in contrast to the 169.07 μm path length difference of MZI6.

The experimental results for MZI6 show that the switching temperature is at 50°C. However, this switching temperature is not ideal for real-world applications due to it being quite high. Therefore some design parameters should be changed to make it more feasible. Increasing the path length difference may result in lower temperatures needed to exhibit the same switching mechanisms.

From the comparison of MZI4 and MZI6, we are also able to observe the effect that path length difference has on transmission. It is clear that increasing the path length difference reduces the FSR, and this relationship holds true to equation 1. Although the difference is not stark, it also seems as if having a larger bend radius slightly increases the noise in the transmission curve. MZI6 has approximately 10 dB more TIL than MZI4, and this is most likely due to the combination of having more bends and a much smaller bend radius.

Due to the nature of fabrication, there will always be some variability between devices that are supposed to be identical. Unfortunately, identical devices were not designed for this report; however, fabrication variability can introduce defects or imperfections between the devices. These would have effects on the overall transmission of the devices which could include shifts or changes in amplitude of transmission graphs. From observing the transmission graphs, we can also see that there is still lots of noise at certain wavelengths. This may be due to either fabrication imperfections or impurities nested in the waveguides.

This report presents the design and experimental results of an MZI with a thermo-optic switching mechanism, and compares it to the simulation data. From the experimental data of this MZI, we are able to confirm that the original design specifications from simulations still hold true. We show that the wavelength dependence on temperature for this MZI is approximately 0.07 nm/°C and that the π phase shift required for switching occurs with a 25°C increase from room temperature. When comparing MZIs with various path length differences, we can also see how the FSR becomes larger as path length difference is decreased. Significant improvements in the design process can be made, because the original specifications were not used in the actual implementation of the devices. More variations of the simple devices would be required as well to determine loss from individual components like the VGCs and Y-branches. In future work, the design of different devices to be used as optical switches would be interesting to explore.

References

[1] Richard Soref. The past, present, and future of silicon photonics. *IEEE Journal of Selected Topics in Quantum Electronics*, 12(6):1678–1687, 2006.

[2] Odile Liboiron-Ladouceur. Ecse 596 lecture 6 notes: Fundamentals of waveguide propagation, January 2021.